Applied Ocean Research 52 (2015) 92–101

Contents lists available at ScienceDirect

Applied Ocean Research

journal homepage: www.elsevier.com/locate/apor

A practical approach to predicting cross-flow and in-line VIV response for deepwater risers

Xue Hongxiang[a,b,*], Wang Kunpeng[a,b], Tang Wenyong[a,b]

[a] State Key Laboratory of Ocean Engineering, Shanghai Jiao Tong University, Shanghai 200240, China
[b] Collaborative Innovation Center for Advanced Ship and Deep-Sea Exploration, Shanghai 200240, China

ARTICLE INFO

Article history:
Received 17 October 2014
Received in revised form 11 May 2015
Accepted 19 May 2015

Keywords:
Vortex-induced vibration
Cross-flow
In-line
Riser

ABSTRACT

In this study, a practical model is proposed to predict cross-flow (CF) and in-line (IL) vortex-induced vibrations of a flexible riser in time domain. The hydrodynamic force as a function of non-dimensional amplitude and frequency is obtained from the forced vibration experimental data of a two-dimensional cylinder. An empirical nonlinear damping model is used to simulate the hydrodynamic damping outside the experiment's range. Coupling effect of CF and IL-VIV is taken into account by implanting a magnification model for the IL hydrodynamic force associated with CF amplitude, and by increasing the non-dimensional amplitude corresponding to the IL hydrodynamic coefficient in the second excitation region. The experimental models of flexible riser under the uniform and sheared current are simulated to validate the proposed model. The predicted displacement, curvatures, excited modes and fatigue damage show reasonable agreement with the measured data.

1. Introduction

Deepwater riser is an important component of oil and gas exploration and production system. When ocean current crosses, vortex would shed periodically at the two side of the riser, which leads to riser vibration, i.e. vortex-induced vibration. When riser response is locked in vortex shedding frequency, VIV amplitude would increase obviously, which would cause severe fatigue damage. This problem becomes more crucial in riser design as oil and gas exploration and production moves to deeper water.

Cross-flow (CF) VIV has been studied for several decades. Nowadays, the frequency domain codes, such as SHEAR7 [1] and VIVANA [2], have been widely used, and are sophisticated to predict CF-VIV response for riser's engineering design by using large safety factor. As for in-line (IL) VIV aligned with current, only few woks have been undertaken during the recent years, and are mainly based on frequency domain prediction approach and laboratory test [3–5]. Baarholm et al. [6] show that, although the in-line amplitude is less than cross-flow response, the fatigue damage induced by IL-VIV is almost the same to CF-VIV due to higher dominant frequency about twice of cross-flow response, therefore IL-VIV should not be negligible in deepwater riser design.

Frequency domain approach costs efficiently, and suits for preliminary design. However, frequency domain approach cannot account for the variation of current, the interaction between riser and keel guides of the hull, and the soil–SCR interaction. Therefore, some researchers focus on time domain approach for CF-VIV prediction. Chang and Isherwood [7] developed a time domain VIV prediction code using wake-oscillator model and vortex tracking model. Srinil [8] simulated Tognarelli's laboratory test model [9] using wake-oscillator model by assuming the riser response frequency locked in the Strouhal frequency associated with the maximum current velocity. Cheng et al. [10,11] carried out lots of validation works using different riser models. Sidarta et al. [12] developed VIV time domain prediction code, SimVIV, which used the lift coefficient in SHEAR7. Wang et al. [13] used the forced vibration test data to predict CF-VIV of a riser test model carried out by Chaplin et al. [14,15] in time domain and the fatigue damage of steel catenary riser near touchdown point was predicted by the numerical approach [16]. Thorsen et al. [17,18] proposed a phase model of fluid force based on the CF forced vibration test data of rigid cylinder. The proposed model is tested by numerical simulations, and the results are compared to experimental observations.

The studies mentioned above are mainly focus on CF-VIV, while coupled analysis of CF and IL-VIV in time domain is mostly limited to elastically supported rigid cylinder. Jauvtis and Williamson [19], Stappenbelt et al. [20] and Blevins and Coughran [21] carried out a series of rigid cylinder VIV tests and obtained the coupled response characteristics of CF and IL-VIV. Srinil and Zanganeh [22] proposed an approach using wake-oscillator model to simulate the CF and

* Corresponding author at: State Key Laboratory of Ocean Engineering, Shanghai Jiao Tong University, Shanghai 200240, China. Tel.: +86 21 34204968.
E-mail address: hongxiangxue@sjtu.edu.cn (H. Xue).

0141-1187/$ – see front matter © 2015 Elsevier Ltd. All rights reserved.
http://dx.doi.org/10.1016/j.apor.2015.05.005

IL-VIV of rigid cylinder mounted elastically. Sumer and FredsØe [23] highlighted that when CF-VIV amplitude exceeds 0.2–0.3 times cylinder's diameters, the in-line excitation force would be significantly magnified. Since most of the previous studies and numerical codes mentioned above mainly focus on cross-flow vibration, and do not include the prediction of in-line response. Therefore, a prediction model accounting for both cross-flow and in-line vibrations, as proposed in the present study, would be worthwhile from a practical and industrial viewpoint.

In this paper, a practical approach for cross-flow and in-line VIV analysis of deepwater riser is proposed. The forced vibration experimental data of the rigid cylinder is used to simulate the cross-flow and in-line hydrodynamic coefficient respectively. Outside the test region of non-dimensional VIV amplitude and frequency, the empirical damping model which can include the effects of oscillation frequency, vibration amplitude, cross-section properties and local flow velocity is used. Considering the coupling effect, the in-line hydrodynamic force is corrected by a magnification coefficient related to CF response. In order to validate the approach, two flexible riser models under the uniform and sheared current are simulated respectively, and the numerical results are reasonable compared to the measured data.

2. VIV hydrodynamic force model

Deepwater riser has a large aspect ratio of length to diameter. Therefore, by considering the riser as a flexural elastic structure satisfying the Euler–Bernoulli beam hypothesis, the governing differential equation for a riser could be expressed as Eqs. (1) and (2) in the Cartesian coordinate system with x-axial and y-axial, aligned with and transverse with current velocity respectively, and z-axial upwards. It is assumed that the current speed is constant.

$$\text{In-line direction}: \quad m\frac{\partial^2 x}{\partial t^2}+c\frac{\partial x}{\partial t}+EI\frac{\partial^4 x}{\partial z^4}-\frac{\partial}{\partial z}\left(T\frac{\partial x}{\partial z}\right) = F_x(A^*_{CF}, A^*_{IL}, f_{r,IL}) \tag{1}$$

$$\text{Cross-flow direction}: \quad m\frac{\partial^2 y}{\partial t^2}+c\frac{\partial y}{\partial t}+EI\frac{\partial^4 y}{\partial z^4}-\frac{\partial}{\partial z}\left(T\frac{\partial y}{\partial z}\right) = F_y(A^*_{CF}, f_{r,CF}) \tag{2}$$

where m is riser's mass per unit length, c is the structural damping, E is the elastic modulus, I is the moment of inertia, T is the effective tension, $F_x(A^*_{CF}, A^*_{IL}, f_{r,IL})$ and $F_y(A^*_{CF}, f_{r,CF})$ are hydrodynamic forces in IL and CF direction respectively, A^*_{IL} and A^*_{CF} are the IL and CF non-dimensional response amplitude to diameter D, $f_{r,IL}=f_{IL}D/V$ and $f_{r,CF}=f_{CF}D/V$ are the non-dimensional frequency, and V is the current velocity.

The hydrodynamic forces F_x and F_y can be decomposed into one component in phase with riser's velocity, excitation force F_V, and another component in phase with riser's acceleration, inertia force F_M, which both depend on response amplitude, oscillation frequency and current velocity. Assuming that the exciting force acting on riser segment following sinusoidal in one period, the hydrodynamic force in both directions could be expressed as:

$$F_V=\frac{1}{2}f_{amp}(A^*_{CF})C_{V,IL}(A^*_{IL}, f_{r,IL})\rho_f DV^2\ \sin(2\pi f_{IL}t)$$

In-line direction :

$$F_M=-m_{a,IL}\frac{\partial^2 x}{\partial t^2} \tag{3}$$

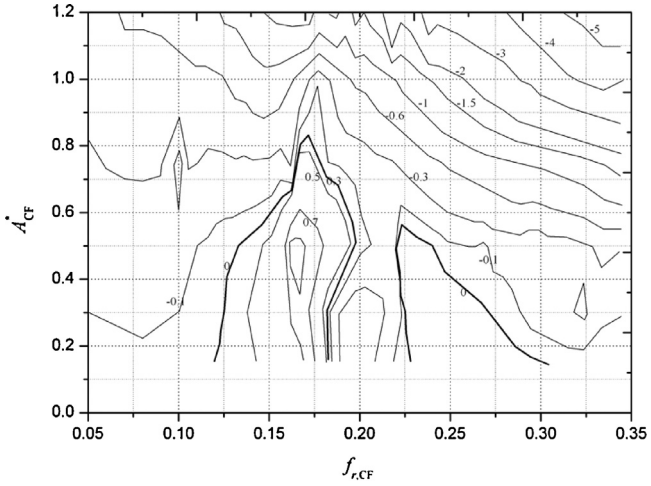

Fig. 1. CF excitation coefficient.

$$F_V=\frac{1}{2}C_{V,CF}(A^*_{CF}, f_{r,CF})\rho_f DV^2\ \sin(2\pi f_{CF}t)$$

Cross-flow direction :

$$F_M=-m_{a,CF}\frac{\partial^2 y}{\partial t^2} \tag{4}$$

where $C_{V,IL}$ and $C_{V,CF}$ are the lift coefficients. f_{amp} is the magnification coefficient due to CF-VIV, ρ_f is the fluid density, $m_{a,IL}$ and $m_{a,CF}$ are the added mass per unit length in in-line and cross-flow direction respectively. In CF- and IL-VIV, the added mass coefficient is a function of non-dimensional frequency. For simplification as SHEAR7 [1], this study takes it to be 1.0.

Gopalkrishnan [24] carried out a series of cylinder forced vibration test in towing tank, and obtained the contour of $C_{V,CF}$. Several years later, by forcing the cylinder oscillating in in-line direction, Aronson and Larsen [4] obtained the $C_{V,IL}$ contour. Figs. 1 and 2 are the contours of excitation coefficient of CF-VIV and IL-VIV respectively. Fig. 1 shows that cross-flow VIV excitation bandwidth can be defined as a single interval around $0.125 < f_{r,CF} < 0.20$. Differing from CF-VIV, there exist two main excitation regions for in-line vibration. Fig. 2 indicates that the first region is around $0.375 < f_{r,IL} < 0.76$ which is caused by the combined action of normal vortex shedding giving rise to two oscillations per shedding and symmetric vortex shedding which occurs as a result of in-line motion of the

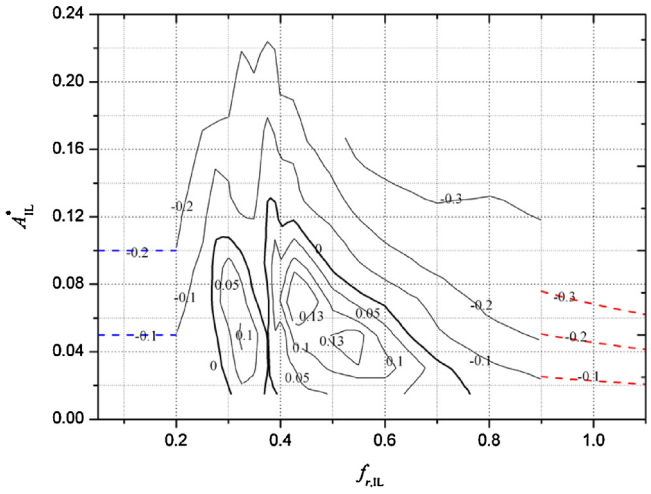

Fig. 2. IL excitation coefficient.

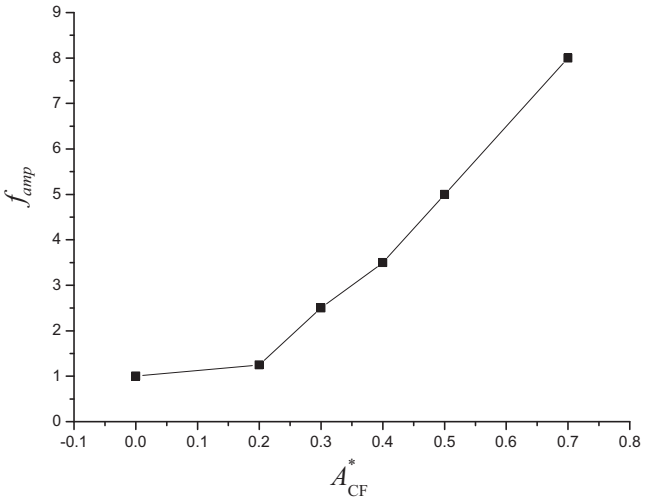

Fig. 3. In-line excitation amplification factor.

riser relative to the fluid. The lift force in this region is assumed to be associated with a vortex shedding frequency corresponding to three times the Strouhal number, i.e. $f_s = 3S_tV/D$, where f_s is the shedding frequency and S_t is the Strouhal number. The second excitation region is around $0.27 < f_{r,IL} < 0.375$, and only normal vortex shedding dominates the riser's response, so the vortex shedding frequency is corresponding to two times the Strouhal number, i.e. $f_s = 2S_tV/D$. Actually, observations show that there may exists the third excitation region. In this region, in-line VIV excitation occurs together with the cross-flow VIV excitation. Due to the reason that the forced vibration experiments are pure in-line VIV, and the hydrodynamic coefficients of this region cannot be obtained. Hence, only the first and the second excitation region as shown in Fig. 2 are considered in this study.

Jauvtis and Williamson [19] and Goncalves et al. [25] showed that when CF-VIV is locked in, the non-dimensional frequency of in-line response is approximate in the second excitation region. Additionally, when the cross-flow non-dimensional amplitude exceeds 0.2–0.3, the in-line excitation force would be magnified obviously. The magnification coefficient as a function of cross-flow amplitude proposal by Sumer and FredsØe [23] is shown in Fig. 3.

If the excitation coefficient is positive, the excitation force will synchronize to the riser's velocity, and the power will be translated from fluid to the riser. However, if negative, damping force will act on the riser, and the damping coefficient can be obtained by assuming equivalent power dissipated in an oscillation period:

$$c_f = -\frac{C_V \rho_f V^2 D}{2A\omega} \tag{5}$$

Outside the experimental data range, an empirical damping model for CF-VIV proposed by Venugopal [26] is used to simulate the hydrodynamic damping. The nonlinear damping model is able to handle the damping force affected by the contributing factor such as actual oscillation frequency, vibration amplitude, cross-section properties and local flow velocity.

Damping in high non-dimensional frequency regions:

$$c_f = C_{lf}\rho_f DV + c_{sw} \tag{6}$$

where $C_{lf} = 0.18$. c_{sw} is the still water damping given by:

$$c_{sw} = \frac{\omega\pi\rho_f D^2}{2}\left[2\sqrt{\frac{2}{\omega D^2/\nu}} + C_{sw}\left(\frac{A}{D}\right)^2\right] \tag{7}$$

where ν is the kinematic viscosity of the fluid, and $C_{sw} = 0.25$.

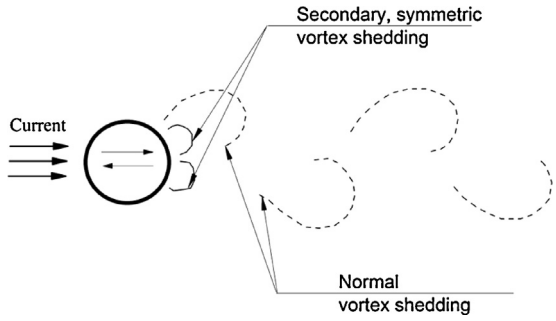

Fig. 4. Sketch of shedding vortex modes.

Damping in low non-dimensional frequency regions:

$$c_f = \frac{C_{hf}\rho_f V^2}{\omega} \tag{8}$$

where $C_{hf} = 0.2$.

The above damping model is also used for IL-VIV with different empirical coefficients due to the oscillation direction and vortex shedding mode. By compared to the extension of $C_{V,IL}$ curve, C_{lf} is set to 0.35, C_{hf} set to 1.0. Fig. 2 gives the excitation coefficient extended curve calculated by the damping model.

3. Lock-in regime

Figs. 1 and 2 show that amplitude and oscillation frequency are key factors to determine the hydrodynamic force. So at each step, riser's displacement and velocity should be extracted to calculate the amplitude and frequency. In this study, the calculated frequency consisting of multi-modal frequencies is not used to obtain the hydrodynamic force directly, but to determine the Strouhal number and the dominant frequency for each numerical element, which also has relationship with the excitation bandwidth. It is assumed that the dominant frequency is the oscillation frequency, f_{osc} when calculating the hydrodynamic force for each numerical element.

For CF-VIV, the non-dimensional frequency with a range from 0.125 to 0.20 is selected to determine the excitation bandwidth, which is to be corrected for variations of Strouhal number, see Eq. (9). If the calculated non-dimensional frequency is within the excitation bandwidth, it will be locked onto the riser natural frequency closer to the value associated with the non-dimensional frequency of 0.17 corresponding to largest excitation coefficient. Outside the excitation bandwidth, the calculated frequency is used to obtain hydrodynamic coefficient.

$$\left(\frac{f_r}{S_t}\right)_{test} = \left(\frac{f_r}{S_t}\right)_{actual} \tag{9}$$

Differing from CF-VIV, there are two excitation regions in in-line direction. The non-dimensional frequency is from 0.375 to 0.76 for the first region, and is from 0.27 to 0.375 for the second region, as shown in Fig. 2. The response corresponding to the first region is caused by the combined action of normal vortex shedding giving the riser two oscillations per shedding, and secondary, symmetric vortex shedding which occurs as a result of in-line motion of the riser relative to the fluid. If the non-dimensional frequency falls in the second region, only normal vortex shedding dominates riser response. Fig. 4 gives the sketch of in-line vortex shedding.

It is assumed that two riser natural modes falling in the different excitation region are independent. The following gives the determination of in-line dominant frequencies:

(1) Assuming that the non-dimensional frequencies of 0.43 and 0.33 are the power-in center for the first and second excitation

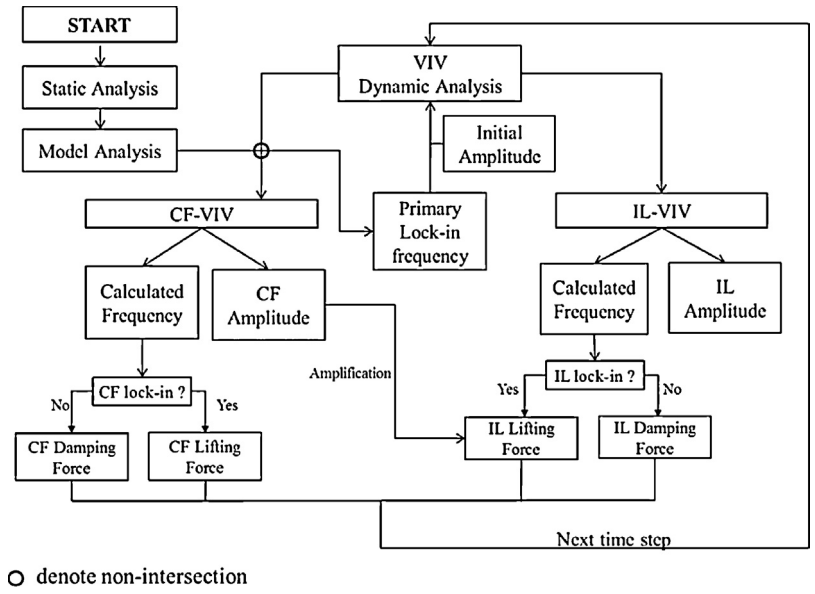

Fig. 5. Flow chart of VIV analysis.

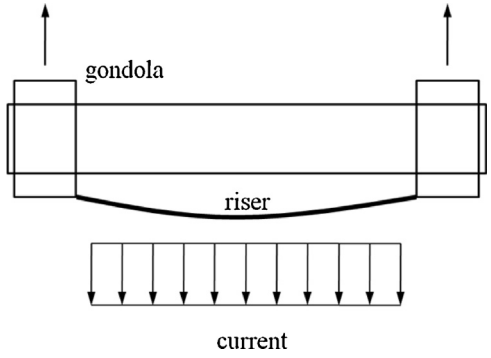

Fig. 6. Trim's experiment set-up.

region respectively, the natural frequencies closer to the power-in centers are obtained.

(2) If the calculated non-dimensional frequency is within the range from 0.27 to 0.76, the above two natural frequencies will dominate the riser element response. Outside the range, the calculated frequency is considered as dominant frequency as well as CF-VIV.

If the riser element is dominated by two different modes, the calculated amplitude is divided to them according to the criterion of maximum combined excitation force. The time domain analysis flow is shown in Fig. 5 to better demonstrate the proposed approach.

Table 1
Parameters of Trim's riser models.

Parameters	Value
Length (m)	38
Out diameter (m)	0.027
Inner diameter (m)	0.021
Young's modulus (Pa)	3.62×10^{10}
Mass ratio	1.6
Structural damping	0.003
Top tension (N)	5000

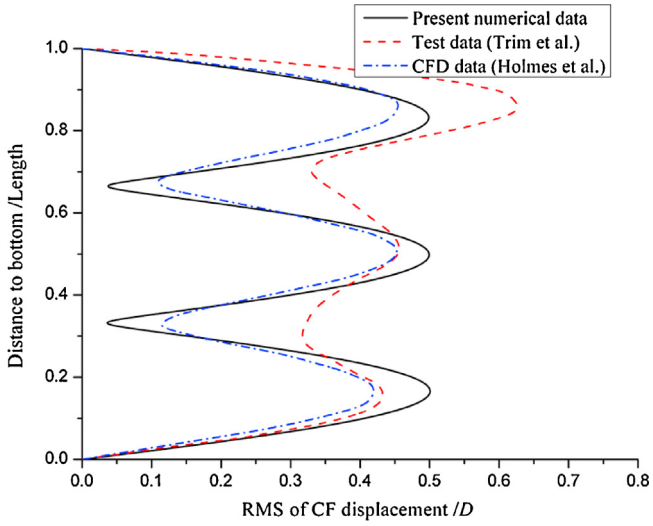

Fig. 7. RMS of CF displacement.

4. Validation against laboratory experiment

4.1. Tensioned risers in a uniform current

In Trim's experiment [27], uniform current was simulated by towing the gondola in one direction using the crane. Fig. 6 is the layout of the riser model. The parameters of the riser are listed in Table 1.

The case with current velocity of 0.4 m/s is calculated. The envelopes of the RMS displacement A/D along the riser for CF and IL-VIV are shown in Figs. 7 and 8 respectively. For CF-VIV response, the present method predicts the same main excited mode and the approximate amplitudes as well as the experimental data and the CFD results by Holmes and Owen [28]. For IL-VIV, the present method predicts mode 5 as the main excited mode, showing better comparison to the experimental data than CFD results. Fig. 8 also demonstrates the significant effect of the CF-VIV on the IL-VIV. It can be found that if the amplification effect is neglected, the IL-VIV will be severely underestimated.

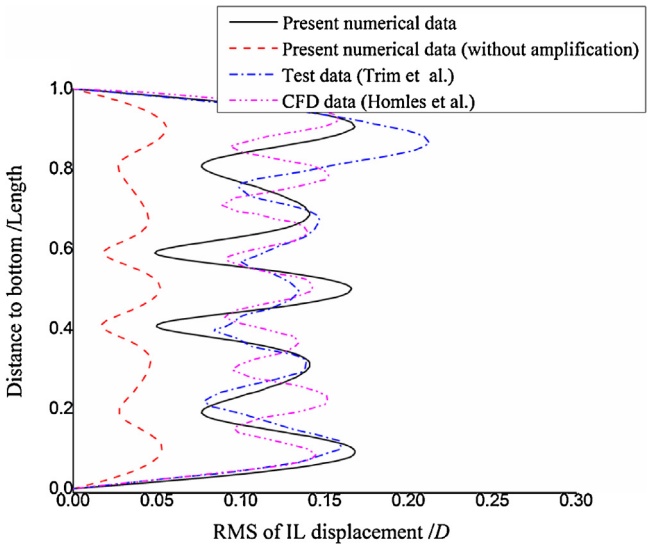

Fig. 8. RMS of IL displacement.

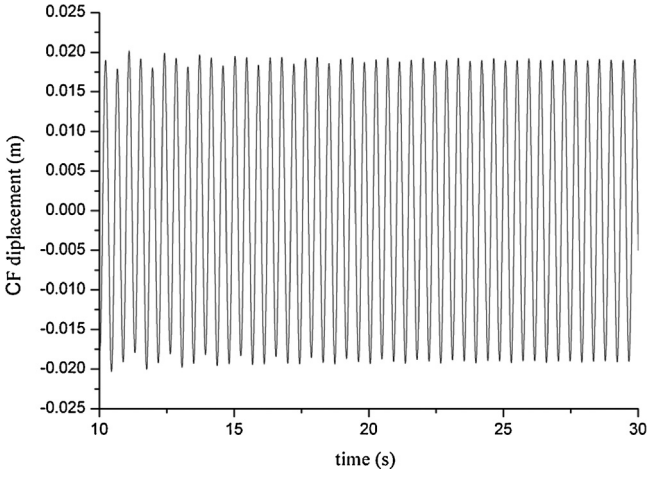

Fig. 9. CF-VIV displacement of midpoint.

Figs. 9 and 10 are the response history of the riser's midpoint for the two directions, which have been extracted the static displacement due to in-line current. It can be found that CF-VIV is obviously single-mode dominated, whereas IL-VIV shows irregular response in uniform current.

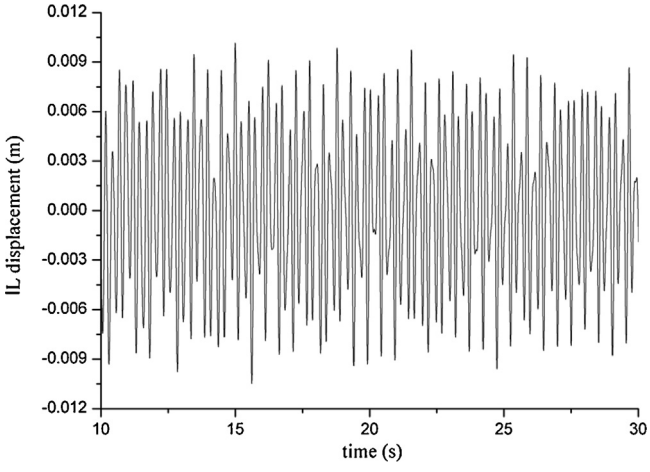

Fig. 10. IL-VIV displacement of midpoint.

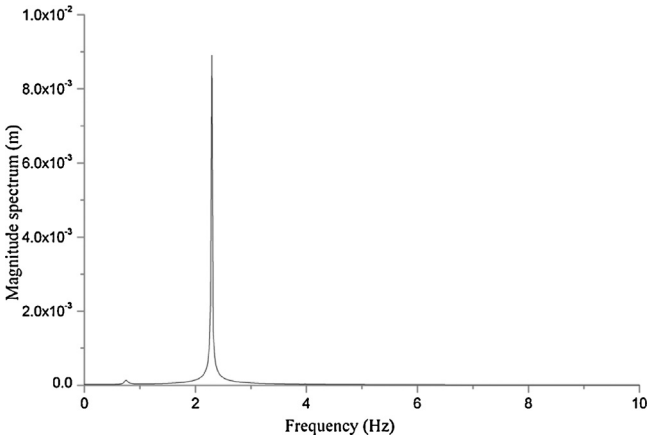

Fig. 11. CF-VIV amplitude spectrum of midpoint.

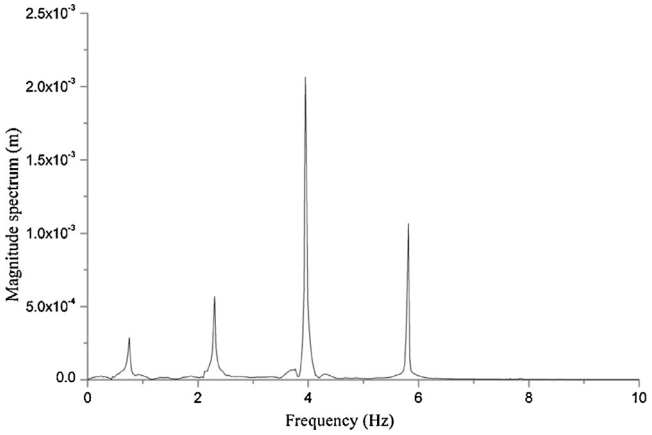

Fig. 12. IL-VIV amplitude spectrum of midpoint.

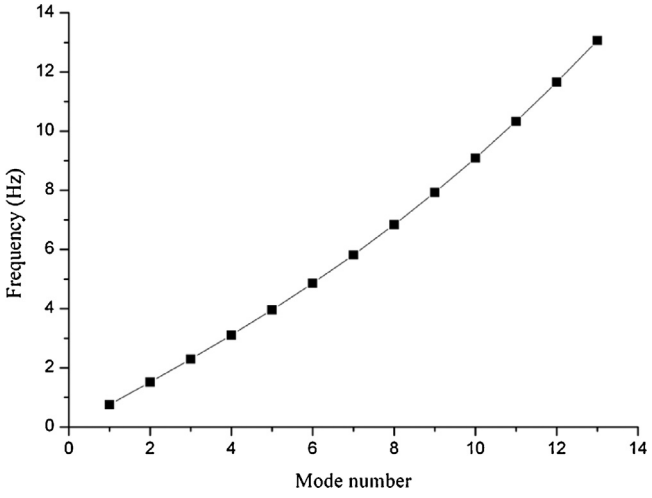

Fig. 13. Natural frequency of the riser in Trim's experiment.

According to Figs. 11 and 12, IL dominant frequency is about double CF frequency. Additionally, a mode with triple frequency of CF-VIV would be extensively excited in in-line direction, which corresponds to the first excitation region. Due to the coupling effect, IL-VIV response would have a component associated with CF-VIV dominant frequency; the fundamental mode would be slightly excited in CF and IL direction, whose frequency is shown in Fig. 13.

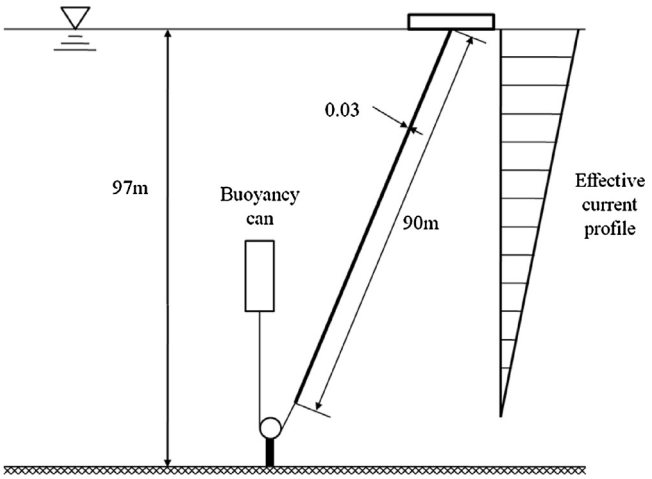

Fig. 14. Configuration of the experiment at HanØtangen.

Table 2
Parameters of HanØtangen's riser model.

Parameters	Value
Length (m)	90
Out diameter (m)	0.03
Inner diameter (m)	0.026
Young's modulus (Pa)	2.1×10^{11}
Mass ratio	3.13
Structural damping	0.003
Top tension (N)	3700

4.2. Tensioned risers in a linearly sheared current

In this section, the proposed method is to be validated by tensioned risers in sheared current. HanØtangen's experiment was carried out on the west coast of Norway. The 90 m riser model was attached to a floating vessel and kept at constant tension by a buoyancy can, as shown in Fig. 14 [29]. By moving the vessel at a constant speed, the riser was exposed to a linearly sheared current. The parameters of the riser are presented in Table 2.

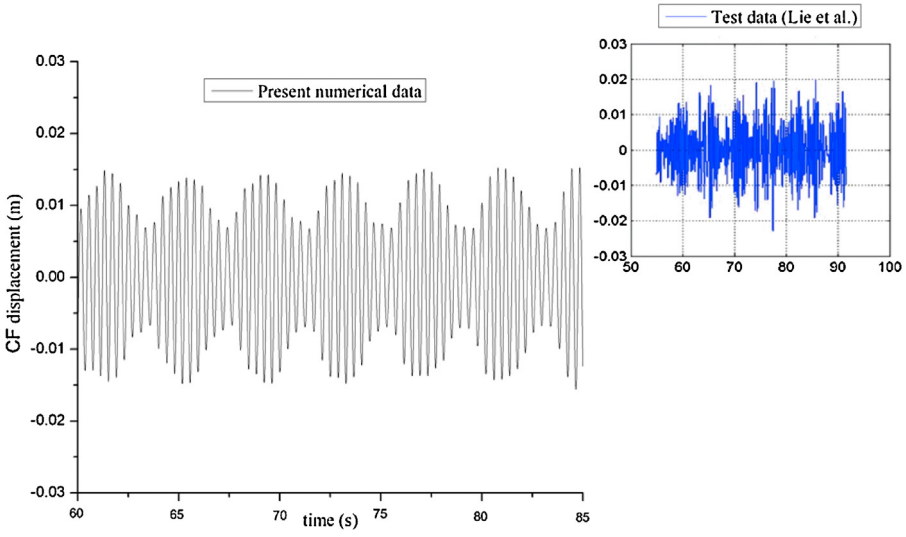

Fig. 15. CF-VIV displacement of midpoint.

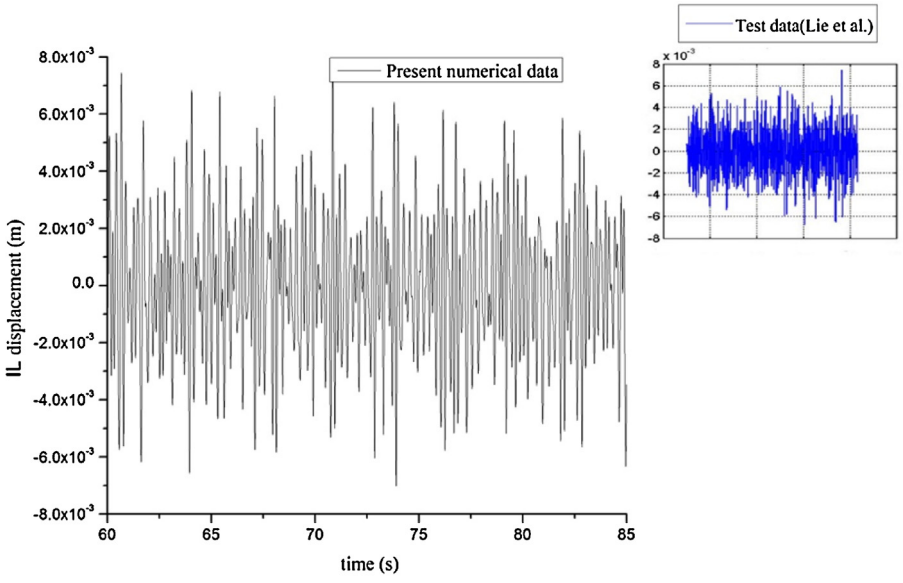

Fig. 16. IL-VIV displacement of midpoint.

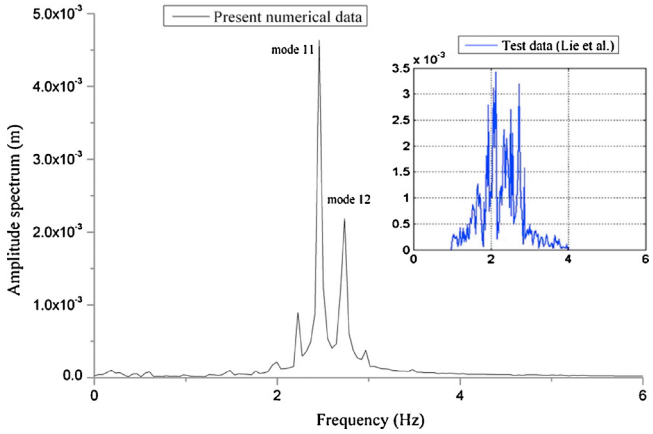

Fig. 17. CF-VIV amplitude spectrum of midpoint.

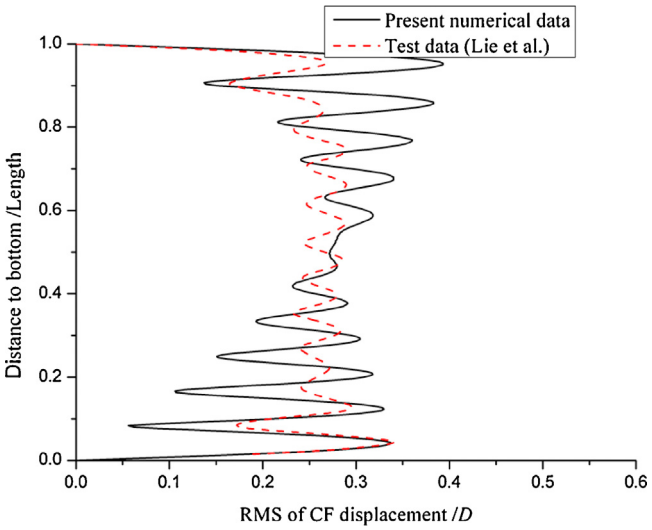

Fig. 19. RMS of CF displacement.

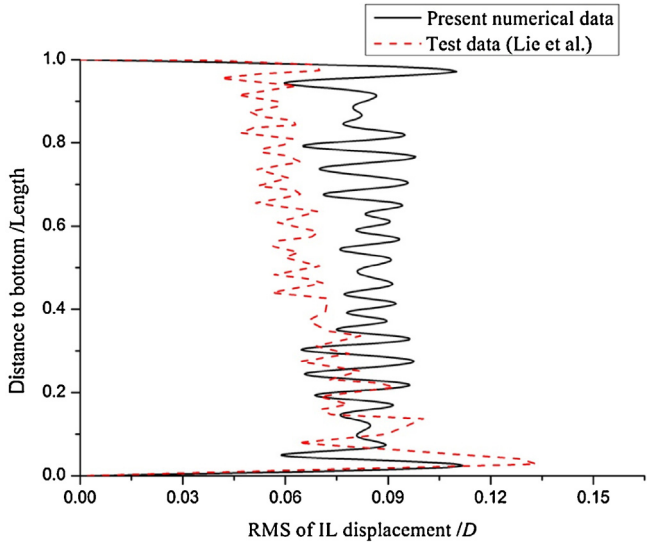

Fig. 20. RMS of IL displacement.

The case with top velocity of 0.54 m/s is calculated by the proposal numerical model. Figs. 15 and 16 are the time history of displacement of riser midpoint in CF and IL directions respectively, which have been extracted the static displacement due to in-line current. The ranges of the present predicted data and the experimental data are both approximate from −0.015 m to 0.015 m for CF-VIV, and from −0.006 m to 0.006 m for IL-VIV.

According to the time history above, FFT is used to obtain the amplitude spectrum. Fig. 17 illustrates that the bulk of the CF response of the present model and the experimental measurement are mainly exists between 2 and 3 Hz. The experimental data shows two highest peaks at 2.1 and 2.7 Hz, whereas highest peak of the present results occurs at about 2.4 Hz associated with mode 11.

In Fig. 18, it can be found that more and higher modes are excited in IL-VIV, which makes the IL response much more irregular than CF direction. The measured participating mode numbers are from 10 to 29, slightly higher than the predicted results, which are from 9 to 27.

Fig. 19 shows the RMS displacement in cross-flow direction. According to the amplitude spectrum predicted using the present model in Fig. 17, the amplitude of mode 11 is obviously larger than that of mode 12. However, the variation trend of the envelopes along the riser indicates that the present model predicts mode 12

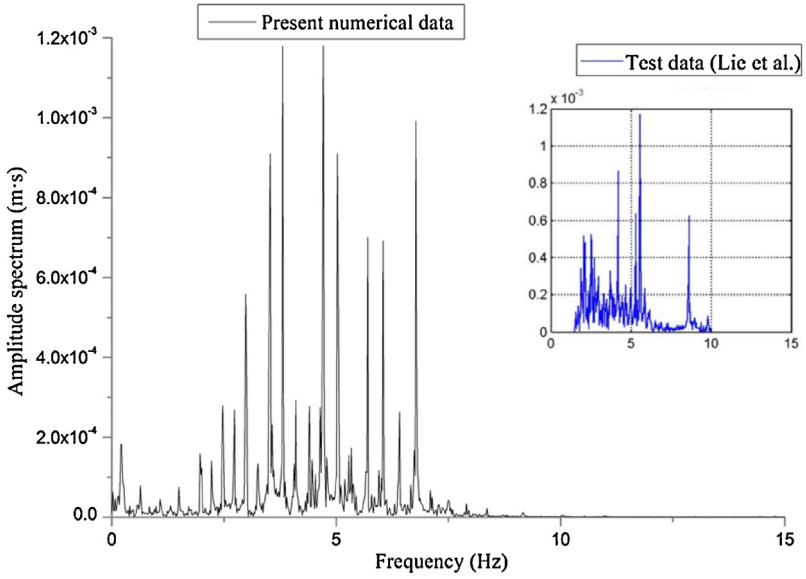

Fig. 18. IL-VIV amplitude spectrum of midpoint.

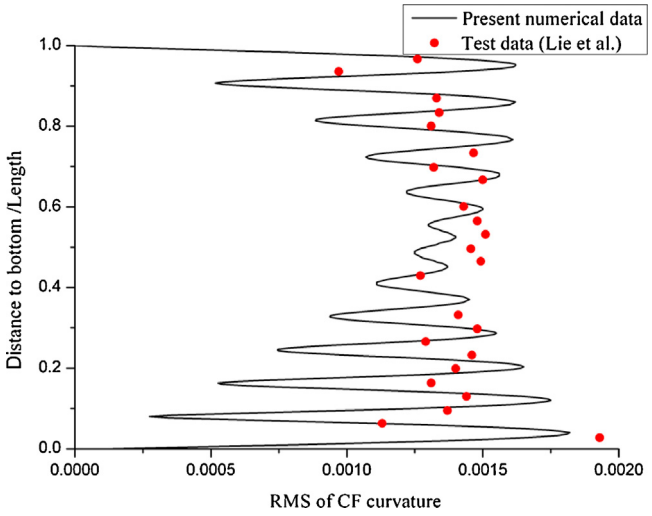

Fig. 21. RMS curvature of CF-VIV.

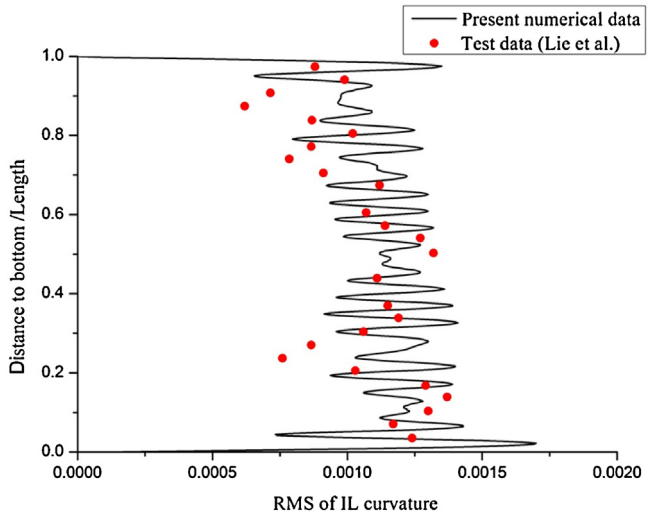

Fig. 22. RMS curvature of IL-VIV.

as the dominant mode, which is little larger than the experimental results, especially near the top of the riser. The RMS of in-line displacement is shown in Fig. 20. Although the present model gives lower dominant mode than the test model, they predict approximate average RMS displacement.

Figs. 21 and 22 show the comparison of curvature along the riser in CF and IL directions. The results show that in the mid region of the riser, the present model predicts little lower CF curvatures, and in the two end regions, the curvature values are approximate with the experimental data. It should be noted that curvature is proportional to bending stress while calculating structural fatigue damage. The curvatures in CF and IL are at the same level for this large scale riser model, so it can be drawn that IL-VIV should not be neglected for deepwater riser's design.

For more convincing, the present study chooses four cases to calculate the CF and IL VIV induced fatigue damages using rain flow counting methodology. The corresponding top velocities are: 0.37 m/s, 0.64 m/s, 1.06 m/s and 1.37 m/s. The S–N curve parameters were presented in Baarholm et al. [6]. The average RMS displacement and peak frequency at riser midpoint are compared with the experimental data in Figs. 23 and 24. The former shows good agreement, while the latter is overestimated. Noted that the experimental data associated with top velocity equal to 1.37 m/s is not

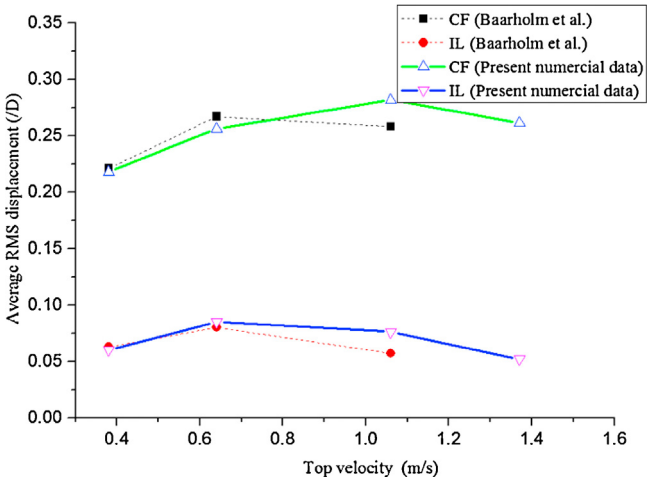

Fig. 23. Comparison of CF and IL VIV induced average RMS displacement.

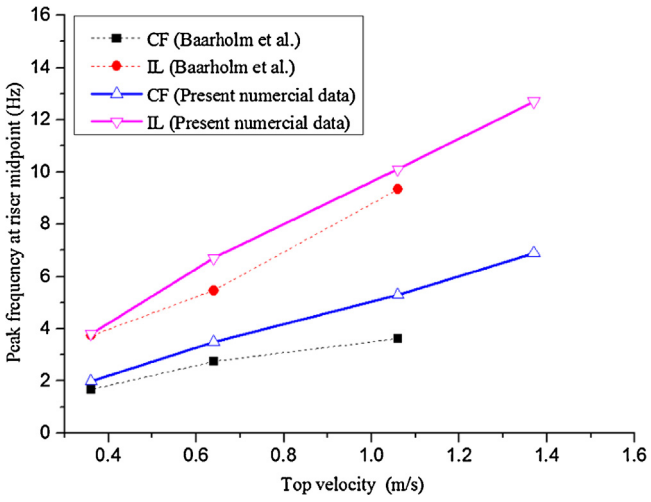

Fig. 24. Comparison of CF and IL VIV induced peak frequency at riser midpoint.

plotted since it is not provided in the literature. Figs. 25 and 26 illustrate the CF and IL VIV induced fatigue damage profiles along the riser under top velocity equal to 0.64 m/s. For CF VIV, the present approach overestimates the fatigue damage at the riser top, while

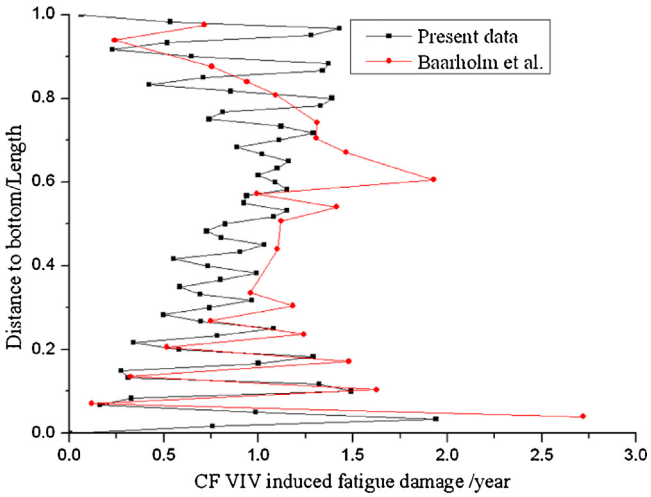

Fig. 25. Comparison of CF VIV induced fatigue damage under top velocity equal to 0.64 m/s.

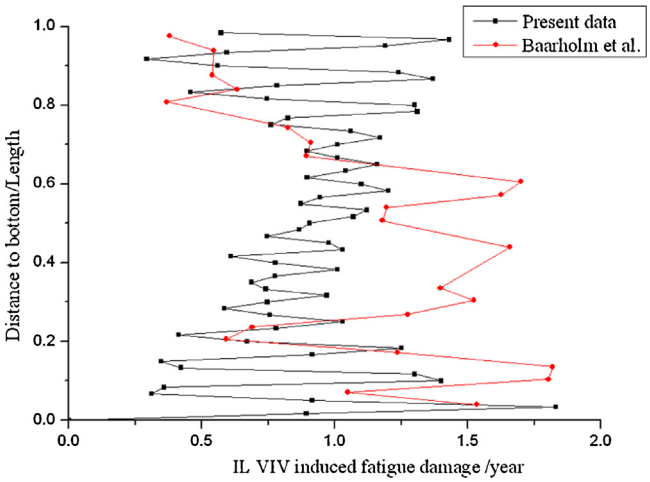

Fig. 26. Comparison of IL VIV induced fatigue damage under top velocity equal to 0.64 m/s.

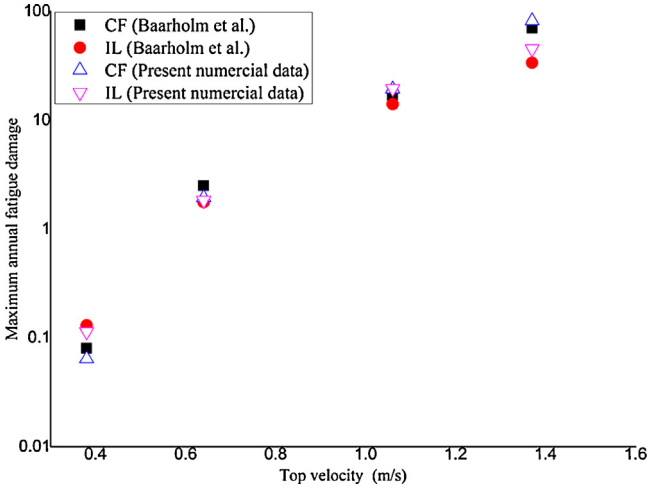

Fig. 27. Comparison of maximum fatigue damage under different top velocities.

underestimate the fatigue damage at the riser bottom. For IL VIV, the present approach also overestimates the fatigue damage at the riser top, while underestimates the fatigue damage at riser middle. Overall, the predicted results are reasonable. Fig. 27 demonstrates the maximum fatigue damage along riser under different top velocities. It is shown that the predicted maximum fatigue damage shows good agreement with the test data and the present approach can well predict the fatigue damage at a wide range of current velocity.

5. Conclusions

A practical time domain model of predicting VIV response in cross-flow and in-line directions for deep water riser is developed. In this approach, the hydrodynamic coefficients depended on the non-dimensional amplitude and frequency obtained by forced vibration experimental data are used, and extended by empirical damping model. The coupling effect of CF and IL-VIV is taken into account, and the dominant frequency is depended on the natural frequency. By simulating two experimental models, the present model is validated, and some conclusions are obtained:

(1) The envelopes of RMS displacement along the riser show good agreement with the experimental data in CF and IL directions except for the regions around two ends. Compared with the CFD results, the present model shows more sophisticated, and more time efficient.
(2) The agreement between predictions of curvatures and observations is in general good. Additionally, the present study again demonstrates that the in-line curvature is at the same level with the CF-VIV, and highlights the importance of IL-VIV for deep water riser's fatigue analysis.
(3) The bandwidth of amplitude spectrum and the dominant mode are almost the same with experimental data. In the uniform current, the CF-VIV in general shows single-mode response, and IL-VIV is mainly dominated by two modes corresponding to the first and second excitation region respectively. However, in the linearly sheared current, the CF-VIV and IL-VIV both show a certain bandwidth of excited frequency, and have more irregular response.
(4) Although the present approach may not well capture the local fatigue damage features, the predicted results are reasonable from the perspective of the whole riser, and the maximum fatigue damages also show good agreement with the test data at a wide range of current velocities.

The added mass coefficients are assumed to be set as 1.0 in this model for simplifying the analysis. Since the forced vibration test of cylinder showed that the added mass coefficient may be varied with the response amplitude and reduced frequency, further research on this effect is worthwhile.

Overall, the proposed model gives reasonable results for CF and IL-VIV of risers, and can be used as a supplemental approach to overcome the limitation of only predicting CF-VIV in engineering design stage.

Acknowledgements

This paper is based on the projects supported by the National Natural Science Foundation of China (Grant No. 51490674) and Shanghai Municipal Natural Science Foundation (Grant No. 15ZR1423500).

References

[1] Vandiver JK, Li L. SHEAR7 version 4.4 program theoretical manual. Massachusetts, USA: Massachusetts Institute of Technology; 2005.
[2] Larsen CM, Vikestad K. VIVANA – theory manual version 3.4. Trondheim, Norway: Norwegian Marine Technology Research Institute; 2005.
[3] Sidarta DE, Lambrakos KF. A methodology for in-line VIV analysis of risers in sheared currents. In: Proceedings of the 25th international conference on offshore mechanics and arctic engineering. 2006.
[4] Aronson KH, Larsen CM. Hydrodynamic coefficients for in-line vortex induced vibrations. In: Proceedings of the 26th international conference on offshore mechanics and arctic engineering. 2007.
[5] Xue H, Tang W, Qu X. Prediction and analysis of fatigue damage due to cross-flow and in-line VIV for marine risers in non-uniform current. Ocean Eng 2014;83:52–62.
[6] Baarholm GS, Larsen CM, Lie H. On fatigue damage accumulation from in-line and cross-flow vortex-induced vibrations on risers. J Fluids Struct 2006;22:109–27.
[7] Chang SHM, Isherwood M. Vortex-induced vibrations of steel catenary risers and steel offloading lines due to platform heave motions. In: Offshore technology conference. 2003.
[8] Srinil N. Analysis and prediction of vortex-induced vibrations of variable-tension vertical riser in linearly sheared currents. Appl Ocean Res 2011;3:41–53.
[9] Tognarelli MA, Slocum ST, Frank WR. VIV response of a long flexible cylinder in uniform and linearly sheared currents. In: Offshore technology conference. 2004.
[10] Cheng YM, Xu LX. Investigation of VIV fatigue prediction for top tensioned riser. In: Proceedings of the 28th international conference on offshore mechanics and arctic engineering. 2009.

[11] Cheng YM, Lambrakos KF. Time domain VIV prediction for top tensioned risers. In: Proceedings of the 29th international conference on offshore mechanics and arctic engineering. 2010.
[12] Sidarta DE, Finn LD, Maher J. Time domain FEA for riser VIV analysis. In: Proceedings of the 29th international conference on offshore mechanics and arctic engineering. 2010.
[13] Wang K, Tang W, Xue H. Time domain analysis approach for riser vortex-induced vibration based on forced vibration test data. In: Proceedings of the 32nd international conference on ocean, offshore and arctic engineering. 2013. OMAE2013-10285.
[14] Chaplin JR, Bearman PW, Huarte FJH. Laboratory measurements of vortex-induced vibrations of a vertical tension riser in a stepped current. J Fluids Struct 2005;21:3–24.
[15] Chaplin JR, Bearman PW, Cheng Y. Blind predictions of laboratory measurements of vortex-induced vibrations of a tension riser. J Fluids Struct 2005;21:25–40.
[16] Wang K, Xue H, Tang W. Time domain prediction approach for cross-flow VIV induced fatigue damage of steel catenary riser near touchdown point. Appl Ocean Res 2013;43:166–74.
[17] Thorsen MJ, Sævik S, Larsen CM. A simplified method for time domain simulation of cross-flow vortex-induced vibrations. J Fluids Struct 2014;49:135–48.
[18] Thorsen MJ, Sævik S, Larsen CM. Fatigue damage from time domain simulation of combined in-line and cross-flow vortex-induced vibrations. Mar Struct 2015;41:200–22.
[19] Jauvtis N, Williamson CHK. The effect of two degrees of freedom on vortex-induced vibration at low mass and damping. J Fluid Mech 2004;509: 23–62.
[20] Stappenbelt B, Lalji F, Tan G. Low mass ratio vortex-induced motion. In: 16th Australasian fluid mechanics conference. 2007.
[21] Blevins RD, Coughran CS. Experimental investigation of vortex-induced vibration in one and two dimensions with variable mass, damping, and Reynolds number. J Fluids Eng 2009;131(10):101202.
[22] Srinil N, Zanganeh H. Modelling of coupled cross-flow/in-line vortex-induced vibrations using double Duffing and van der Pol oscillators. Ocean Eng 2012;53:83–97.
[23] Sumer B, FredsØe J. Hydrodynamics around cylindrical structures. World Scientific Publishing Company; 2006.
[24] Gopalkrishnan R [Ph.D. thesis] Vortex induced forces on oscillating bluff cylinders. USA: Department of Ocean Engineering, MIT; 1993.
[25] Goncalves RT, Rosetti GF, Fujarra ALC. Experimental comparison of two degrees-of-freedom vortex-induced vibration on high and low aspect ratio cylinders with small mass ratio. J Vib Acoust 2012;134:061009.
[26] Venugopal M [Ph.D. thesis] Damping and response of a flexible cylinder in a current. USA: Department of Ocean Engineering, MIT; 1996.
[27] Trim AD, Braaten H. Experimental investigation of vortex-induced vibration of long marine risers. J Fluids Struct 2005;21:335–61.
[28] Holmes S, Owen HO. Simulation of riser VIV using fully three dimensional CFD simulations. In: Proceedings of 25th international conference on offshore mechanics and arctic engineering. 2006.
[29] Lie H, Kaasen KE. Modal analysis of measurements from a large-scale VIV model test of a riser in linearly sheared flow. J Fluids Struct 2006;22:557–75.